

AD-A086 200

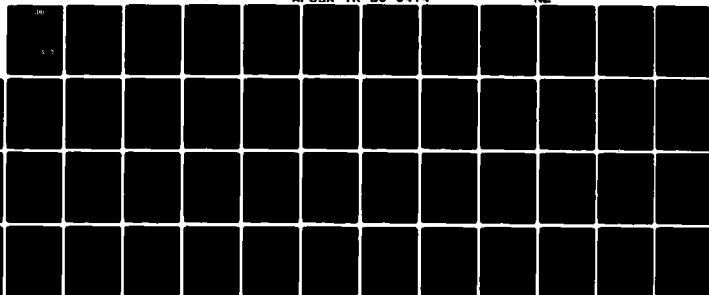
NAPLES UNIV (ITALY) DEPT OF CHEMICAL ENGINEERING F/8 11/4
EFFECT OF APPLIED STRESS, THERMAL ENVIRONMENT AND WATER IN EPOX--ETC(U)
NOV 79 L NICOLAIS, E DRIOLI, A APICELLA AFOSR-77-3369

UNCLASSIFIED

AFOSR-TR-80-0474

NL

AD-A086 200



END

DATE

FILMED

8-80

DTIC

UNCLASSIFIED

SECURITY CLASSIFICATION OF THIS PAGE (When Data Entered)

LEVEL III

AD72701

REPORT DOCUMENTATION PAGE

READ INSTRUCTIONS
BEFORE COMPLETING FORM

1. REPORT NUMBER AFOSR-TR-88-0474	2. GOVT ACCESSION NO. AD-A086 200	3. RECIPIENT'S CATALOG NUMBER (7)
4. TITLE (and Subtitle) EFFECT OF APPLIED STRESS, THERMAL ENVIRONMENT AND WATER IN EPOXY RESINS.		5. TYPE OF REPORT & PERIOD COVERED INTERIM Report 1 Jul 78 - 30 Nov 79.
6. AUTHOR(S) L. NICOLAIS E. DRIOLI A. APICELLA		7. PERFORMING ORG. REPORT NUMBER
8. PERFORMING ORGANIZATION NAME AND ADDRESS UNIVERSITY OF NAPLES DEPARTMENT OF CHEMICAL ENGINEERING NAPLES 80125, ITALY		9. CONTRACT OR GRANT NUMBER(S) AFOSR-77-3369
10. CONTROLLING OFFICE NAME AND ADDRESS AIR FORCE OFFICE OF SCIENTIFIC RESEARCH/NA BLDG 410 BOLLING AFB, DC 20332		11. PROGRAM ELEMENT, PROJECT, TASK AREA & WORK UNIT NUMBERS 2307/B2 61102F
12. MONITORING AGENCY NAME & ADDRESS (if different from Controlling Office) (12) 54		13. REPORT DATE November 1979
		14. NUMBER OF PAGES 33
		15. SECURITY CLASS. (of this report) UNCLASSIFIED
16. DISTRIBUTION STATEMENT (of this Report) Approved for public release; distribution unlimited.		
17. DISTRIBUTION STATEMENT (of the abstract entered in Block 20, if different from Report)		
18. SUPPLEMENTARY NOTES		
19. KEY WORDS (Continue on reverse side if necessary and identify by block number) epoxy resins water and moisture diffusion crazes dual sorption mode plasticization		
20. ABSTRACT (Continue on reverse side if necessary and identify by block number) Because of their elevated physical properties, epoxy resins are widely used as matrices for high performance composites. However, due to moisture induced plasticization and formation of microcavities, high temperature and humidity tend to reduce their physical properties. A history dependent solubility model is generalized in accordance with the Dual Mode Sorption theory to account for effective water diffusion coefficients based on microcavitational damage brought about by temperature and moisture. Laboratory testing for weight changes in sorption-description experiments have been accomplished using a McBain		

DTIC
ELECTE
S JUL 07 1980 D
E

ADA 086200

UNCLASSIFIED

SECURITY CLASSIFICATION OF THIS PAGE(When Data Entered)

↓
quartz-spring microbalance placed in a temperature and humidity controlled cell. Equilibrium moisture absorption levels were represented both by linear and upward isotherms depending upon the humidity history. Analysis of sorption data, using a transport model in which part of the diffusing molecules are completely immobilized in the formed microcavities, revealed the damaging process to be in agreement with the diffusion coefficient depressions and solubility increases predicted by the model. A crazing criterion is qualitatively used to test the nature of the damaging process.
↑

Unclassified

Report number

~~AFOSR-77-3369~~

AFOSR-77-3369

7

EFFECT OF APPLIED STRESS, THERMAL
ENVIRONMENT AND WATER IN EPOXY RESINS

L. NICOLAIS
A. APICELLA
E. DRIOLI

December 1979
Interim Scientific
Report, 01 July 78-
30 November 79

Department of Chemical Engineering,
University of Naples, 80125 Naples,
ITALY

Approved for public release.

Prepared for:

UNITED STATE AIR FORCE, AIR FORCE OFFICE OF
SCIENTIFIC RESEARCH

and

EUROPEAN OFFICE OF AEROSPACE RESEARCH AND
DEVELOPMENT, LONDON, ENGLAND

DTIC
ELECTE
JUL 07 1980
S D
E

Approved for public release:
distribution unlimited.

-1-

Accession For	
NTIS GRA&I	<input checked="checked" type="checkbox"/>
DDC TAB	<input type="checkbox"/>
Unannounced	<input type="checkbox"/>
Justification	
By _____	
Distribution/	
Availability Codes	
Dist	Avail and/or special
A	

ABSTRACT

Epoxy resins are widely used as matrices for high performance composites for their elevated physical properties. However the permanence in a humid environment and at relatively high temperatures produces a reduction of these properties, due to both moisture induced plasticization and microcavities formation. In a previous report the Authors have introduced a simple model to describe temperature history dependence of liquid water sorption in epoxy resin.

A history dependent solubility model is generalized in accordance with the Dual Mode Sorption Theory to take into account a history dependency of effective water diffusion coefficients in epoxy resins, based on a hypothesized microcavitation damage due to the combined effects of temperature and sorbed moisture. For this purpose, weight changes in sorption - desorption experiments, made on thin cast sheets of epoxy resin, have been followed using a Mc Bain quartz - spring microbalance placed in temperature and humidity controlled cell. Attention has been given to the

AIR FORCE OFFICE OF SCIENTIFIC RESEARCH (AFSC)
NOTICE OF TECHNICAL TO 100
This report has been reviewed and is approved for release under E.O. 12958 (7b).
Distribution is unlimited.
A. D. BLOSE
Technical Information Officer

Finally, a crazing criterion is qualitatively used to test the nature of the damaging process involved for the synergistic effects of applied stresses, moisture sorption and temperature. In this first attempt some aspects further indicate crazing as the main phenomenon responsible for the damaging process. The increase of the driving force for cavitation, i.e. applied tensile stress, results in fact in an increase of the apparent solubility. The effects of a hydrostatic compressive stress field is also discussed.

INTRODUCTION

Fiber reinforced plastics are being increasingly utilized for structural applications where their long-term properties are of primary importance. As a result the problem of environmental effects on mechanical performance is attracting a great deal of attention. In the case of epoxy composites it has been shown that their elevated mechanical properties are strongly affected by moisture absorption from high humidity environments (1-9). This effects, especially at higher temperatures, has been associated to moisture induced plasticization and/or micromechanical damaging (6,7). While the plasticization effect is a reversible phenomenon, the microcavitation is not recoverable. The damaging process, governed by synergistic effect of sorbed moisture and temperature, is particularly evident on solubility behaviour, where an additional weight gain is observed (1,3,6) when samples are exposed to cycling conditions of environment and temperature (thermal spikes).

This additional weight gain is attributed to moisture entrapment during microcracking of the resin, since glass transition temperature changes are not observed (6).

Most of the published work is concerned with the combined effects of moisture and temperature on the sorption behaviour of a composite matrix material. In fact, while the sorption process is reasonably well described by classical diffusion laws (1,2,6), history dependent equilibrium moisture solubilities are usually found (1,3,6,10). Sorption behaviour anomalies are particularly apparent at elevated temperatures.

Often, when the diffusing species have high affinity with polymer, the sorption is coupled with molecular relaxation and crazing (11-16) wherein morphological modification of the polymer are involved. Anomalous sorption behaviour has been reported for numerous polymer-diluent systems (13,17,19-22). In the case of thermoplastic polymers, a sharp advancing swollen front has been observed and both the propagation kinetics and the morphological modifications due to the solvent have been extensively studied (18,20-22). Low crosslinked polymers have shown almost similar behaviour (15). However the crosslinked structure of these resins reduces the amount of relaxation due to solvent sorption, which namely may take place

in the regions with low crosslinking density (4,23-25).

Moreover, for moisture and water sorption, localized cavitation has been also associated with the tendency of water to form clusters (12,25).

In the last years interest has been focused primarily on the effects of moisture sorption during "thermal spikes" in real-life simulation tests (1,2,5,6,26,27) on the properties of thermosetting resins. The consequent reduction of ultimate properties has been associated both to irreversible damage (microcracks formation) and to reversible damage (water plasticization) (6). The formed microcavities may trap additional moisture without modifying the total amount of water actually dissolved in the bulk material (i.e. with no further changes in the glass transition temperature (6)). For sorption of gases and vapours in glassy polymers the Dual Mode Sorption Theory has been successfully developed to correlate the presence of hypothesized pre-existing "holes" or "free volume elements" frozen in the glassy state to characteristic sorption behaviours (28-29). Equilibrium weight gains have been described (10) to be progressively affected by microcavity

formation as the temperature was increased.

The history dependent solubility model previously presented is generalized in accordance with the Dual Mode Sorption Theory to take into account a hygrothermal history dependence of effective diffusion coefficient based on induced microcavities. An attempt is made to correlate morphological changes and diffusion parameters in this structurally different material. Sorption kinetics of water and moisture in epoxy resin are here reported and analyzed in sight of a complete immobilization model for trapped species. Equilibrium moisture sorption levels, usually reported to be represented by power law function of the relative humidity with exponents ranging from 1 to 2 or higher values (1,30,31, 27), have been obtained and interpreted in the light of the above model.

SORPTION MODEL

Assuming that the equilibrium concentration of the penetrating species in the glassy polymer may be separated in two terms, one history independent and the other history dependent, one may write:

$$C_T(T, \tau, a, \kappa) = C_1(T, a) + C_2(T, \tau, a, \kappa) \quad (1)$$

where T and a are the actual temperature and external activity, and τ and κ are the previous thermal and activity history. In addition, considering that C_1 may be described by the combination of a Henry's law dissolved term and a Langmuir "preexisting hole filling" term in accordance with the Dual Mode Sorption Theory (28,29), i.e.:

$$C_1 = k_d(T)a + \frac{C'_{ho} b(T) a}{1 + b(T) a} \quad (2)$$

where k_d is the Henry's law constant for dissolved species, a is the external activity and C'_{ho} and b the Langmuir capacity constant for preexisting holes and the affinity constant respectively. Due to the microcavitational nature of the hypotized damage, the history dependent solubility term is assumed to be of Langmuir type only:

$$C_2(T, \tau, a, \kappa) = \frac{C'_h(\tau, \kappa) b(T) a}{1 + b(T) a} \quad (3)$$

where C'_h is the hole saturation constant which is associated with the induced cavities in the polymer and $b(T)$ the polymer-diluent affinity constant, which is the same as the one reported in eq. (2).

Substituting 2 and 3 in one obtains:

$$C_T(T, \tau, a, \alpha) = k_d(T) a + \frac{C'_{ho} + C'_h(\tau, \alpha)}{1 + b(T) a} b(T) a \quad (4)$$

In the case of linear isotherm, where $ab \ll 1$, equation (4) becomes:

$$C_T = [K(T) + K'(T, \tau, \alpha)] a \quad (5)$$

where $K(T) = k_d(T) + C'_{ho} b(T)$ and

$$K'(T, \tau, \alpha) = C'_h(\tau, \alpha) b(T) .$$

For experiments performed at constant temperature and fixed external activity C_T will be only a function of the previous hygrothermal history.

The transport model for systems in which sorbed molecules can be divided in two populations, one formed by completely immobilized molecules and the other by molecules free to diffuse, has been developed by Vieth and Sladek (32) in a modified form of Fick's second law. Subsequently a partial immobilization model has been successfully developed by Paul and Koros (33) from the relaxation of the postulate of complete immobilization suggested by Petropoulos(34). Due to the strong interactions between the penetrant and the polymer and the high cohesive energy of water, large differences in relative mobilities are expected and the total immobilization model has then been used. In such case, in fact, when linear sorption isotherms are experimentally found, diffusion of a penetrant may be described by classic diffusion law with

constant value of the effective diffusion coefficient (35),

$$D_{\text{eff}} = \frac{k_d}{K_T} D \quad (6)$$

where k_d and K_T are respectively the true and the overall apparent Henry's law constant, and D the actual diffusion coefficient of the dissolved species.

Equation 6 states that when part of the diffusing molecules are immobilized, the effective diffusion coefficient is lower than the actual. Once the isotherm 5 is irreversibly fixed by the previous history ($K' = \text{constant}$) is linear and K_T becomes:

$$K_T = K + K' \quad (7)$$

where K and K' are defined in equation 5.

Since k_d can not be directly calculated, equation 6 has been primarily used to investigate the nature of the morphological changes associated with water sorption. In fact, in the case of microcavitational damage, samples damaged by different amounts will show different effective diffusion coefficients and solabilities, also if tested in the same experimental conditions. By indicating with the superscript prime and second the higher and the lower degree of damage respectively, one can write (from equation 6):

$$\frac{D^1}{D^{1'}} = \frac{K^{1'}}{K^{1'}_T} \quad (8)$$

In the case of irreversible microcavitational nature of the damage, equation 8 is verified when for high apparent solubilities, lower effective diffusion coefficients are experimentally found. Moreover classic Fickian diffusion laws for constant diffusion coefficients are not expected to adequately describe water sorption in epoxy resins during the damaging process. This is, in fact, mathematically equivalent to the case of concentration dependent diffusion coefficients, due to the history dependence of K' in equation 6.

EXPERIMENTAL

Materials.

Specimens were prepared from Epikote 828 (kindly supplied by Shell It.) using commercial triethylene-tetramine (TETA) - (Montedison SpA) as curing agent. Distilled water was used in the sorption experiments. Dissolvent gasses were removed by repeated freeze-thaw cycling, under vacuum, using liquid nitrogen as refrigerant. The epoxy samples were prepared following the same procedures previously described (10).

Sorption Kinetics Experiments:

Moisture sorption kinetics and apparent equilibria were determined by means of a Mc Bain (36) quartz, helicoidal spring microbalance served by a standard vacuum system. The quartz springs with a 0.50 mg/mm sensitivity were obtained from the

Ruska Corporation, Worden Quartz Products Division, Houston, Texas. The sample temperature was maintained constant by circulating thermostated water through a water jacket surrounding the sorption cell. Different activities have been maintained in the system by imposing and controlling, by means of a mercury differential manometer, different pressures of water vapors.

Gravimetric liquid sorption measurements were performed by weighing $3.0 \times 3.0 \times 0.05 \text{ cm}^3$ samples repeatedly on a "Galileo" analytical balance following immersion in water maintained at constant temperature. The samples were removed from the water, blotted, placed in a weighing bottle, weighed, and finally replaced in the constant temperature water bath.

Sorption data are indicated as C (percentage of weight gain referred to the dry weight) and plotted as a function of \sqrt{t}/l , where l is the thickness of the samples ranging from 0.2 to 0.4 mm for vapor sorption and from 0.4 to 0.6 for liquid sorption. Sorption equilibria were achieved over 2 to 200 days depending upon the test temperature.

RESULTS AND DISCUSSION

Equilibrium data discussion and presentation of sorption kinetics.

Constant temperature sorptions and desorptions have been carried out on the same sample at progressively higher humidity levels. This will be referred in the following as "First sorption - desorption cycle set" and will be indicated with the Roman numeral I. Once the sample has been equilibrated at the highest humidity level all subsequent sorptions and desorptions will be referred as "Second sorption - desorption cycle set" and it will be indicated by Roman numeral II.

In Figure 1 a) and b) polymer weight gains, expressed as grams of solvent per 100 grams of dry resin, for the first and second sorption - desorption cycle sets at 60° C, have been plotted as a function of square root of time normalized to the sample thickness, l . Numbers on the curves refer to the activity at which the specific test has been performed. The activity is defined as the ratio between the moisture pressure in the sorption cell and the water vapour pressure at the temperature of the experiment. For activities higher than 0.60 first sorption experimental points have not been reported in Figure 1a since the initial part of the curve does not follow the classical Fickian diffusion predictions (37).

The argument will be further developed and discussed in terms of apparent concentration dependence of the "effective" diffusion coefficient in the kinetic paragraph. Conversely in Figure 1b sorption and desorption kinetics have been reported for all activities indicated showing that in this case all the data at low times are correlated by a straight line. In Figure 1c equilibrium solubilities, obtained from the asymptotic values of the sorption curves, both for the first and the second sorption - desorption cycle sets, at different activities, are reported. Open circles refer to the progressive moisture equilibrium weight gains which have been obtained in the first sorption - desorption cycles set. The isotherm is clearly non linear (upward) showing a positive deviation from linearity at higher activities. Once the maximum value of the activity is experienced by the sample, the equilibrium moisture weight gains are linear with the activity values (full circles). The differences in the sorption behaviour, for the same environmental conditions are to be related to a progressive damage that is produced in the material equilibrated at increasingly higher moisture

contents. Once maximum equilibrium moisture content has been reached (in this case $a_{\max} = 0.99$), and the temperature is held at constant value, no additional damage can be induced in the resin. The polymer-water system, then behaves linearly when the internal state of the material does not change during the experiment. In this case an apparent Henry's law constant can be defined as the slope of the linear isotherm. The overall system is then identified by an additional internal state variable which is function of both the temperature and the moisture content. Once the system is fixed the sorption kinetic becomes a reversible phenomenon. In fact the equilibrium values of the solubility for the third sorption - desorption experiments are reported in Figure 1c as full triangles showing a good agreement with the previous data.

The same procedure has been followed for temperatures both higher (75°C) and lower (45°C and 30°C) than the previous one. The first and second sorption - desorption cycle sets are reported in Figures 2a and 2b while humidity history dependent isotherms are shown in Figure 2c for $T=75^{\circ}\text{C}$. The upward isotherm (Fig. 2c) relative to the first sorp-

tion - desorption cycle set equilibrium solubilities (open circles) shows an initial apparently linear part followed by progressive positive deviations for activity higher than 0.60. The existence of this apparently initial linear region indicates that at low moisture contents, independently of the test temperature, the damage induced in the resin is irrelevant. Sorption parameters obtained on "as cast" polymer at low activities can be then referred as relative to the undamaged resin (i.e. K of the solubility model). Again, once the sample has been equilibrated at the highest humidity level ($a = 0.99$), the system behaves linearly for all activities (full circles of Fig.2c) with an overall higher apparent Henry's law constant than in the undamaged state (initial slope of the upward isotherm).

Sorption - desorption cycle sets at 45°C are shown in Figure 3. Additional equilibrium moisture contents for "as cast" samples have been obtained without following the sorption kinetics and are also reported in Figure 3c (open circles).

At this temperature the differences between the linear and the upward isotherms are less pronounced as expected from the temperature dependence of the damage in the resin-water system. Low temperature environment is, in fact, inducing lower damage than a higher temperature environment even in the same conditions of moisture content. When the test temperature was reduced, $T = 30^{\circ}\text{C}$ in Figure 4, a still less pronounced history dependence of the isotherms was found. At this temperature the humidity control was difficult to achieve ($p = 30\text{mm Hg}$) but still appreciable. A dotted line is plotted to indicate the presumed upward isotherm. Once again a linear isotherm is found when samples are previously equilibrated at higher humidity levels. It should be noted that the moisture "per se" is not effective to produce any microcavitation in the resin but, as already pointed out in the literature (1,6), the synergistic effect of moisture and temperature is really effective in the damaging process.

For temperature lower than 30°C (in particular 20°C and 2°C) sorption from liquid phase, $a = 1.00$, has been followed and the data are reported in Figure 5.

In Figure 6 solubilities of resins previously equilibrated at higher humidity levels as function of actual vapour pressures (in mm of Hg) and for different temperatures, as reported on the curves, are shown. For experiments made in the liquid phase, water vapour pressures at the temperature of the tests are used as abscissa. Isotherms are interrupted at pressure values equal to the relative water vapour pressure. The overall apparent Henry's law constants K_T , obtained from Figure 6, are plotted in a van't Hoff diagram in Figure 7 (full circles). On the same figure apparent Henry's law constants for undamaged resin, K_1 , obtained from the initial linear portions of the upward isotherms have also been reported as open circles.

It is interesting to notice that a straight line well correlates the solubility constants data for undamaged resin (low activity test or low temperature experiments), as expected if the upward shape of the isotherm is due to the history dependence of the second term K' of eq. 7 in severe conditions of humidity and temperature. Indeed, if it is so, specimens equilibrated at high humidity levels and at different temperatures are not expected to show apparent

Henry's constants that can be correlated by straight lines in a van't Hoff diagram since they have different degrees of microvoids. However, once the state of the material has been fixed by the hygrothermal history, then a linear relationship must be found. In fact, in Figures 8 a) and b), sorption - desorption curves are reported for tests performed at $T = 30^{\circ}\text{C}$ and $T = 45^{\circ}\text{C}$, respectively, on samples previously equilibrated at $T = 60^{\circ}\text{C}$ and $a = 0.99$. For such system linear isotherms have been obtained and reported in Figure 8c (open circles) together with those obtained on samples equilibrated only at the test temperature (45°C and 30°C) (full circles). It is evident that for systems equilibrated at higher temperature, the higher degree of damage is shown by a higher solubility constant. The overall apparent Henry's constants obtained from Figure 8c and from a low activity test ($a = 0.20$) experiment at 75°C on a previously equilibrated sample at $T = 60^{\circ}\text{C}$ and $a = 0.99$, are reported as full triangles in Figure 7.

As expected, a straight line, parallel to the one corresponding to undamaged resin, well correlates the experimental points.

Concluding, sorbed moisture may induce different degrees of irreversible damage depending upon the temperature and humidity levels imposed on the sample. For low values of temperatures ($T < 20^{\circ}\text{C}$) or for low activities ($a > 0.60$) subsequent sorptions are affected by the previous temperature and humidity histories. History dependent apparent Henry's law constants, as discussed above, give upward shaped isotherms once the damaging process is active.

Conversely, once the damage has reached its maximum value as a result of exposure to drastic environmental conditions (high values of T and a), linear sorption isotherms with higher apparent Henry's law constants are obtained in any subsequent sorption - desorption experiment.

Discussion of kinetic data

Moisture sorption and desorption in epoxy resins have been previously presented for different values of temperature and external activity. Equilibrium moisture sorption levels have been described to be represented, for the same polymer and at the same temperature and humidity conditions, both by linear and upward isotherms (i.e. Fig. 2c), depending upon the humidity history to

which the system was subjected. In first sorptions on "as cast" resins (open circles) the initial apparently linear isotherm (dotted line) was progressively subject to significant positive deviations, associated with a damaging process, as the external activity was increased over 0.60. Once the maximum humidity level imposed to the system is fixed, for all subsequent sorption and desorption, the solubility data were fitted by linear isotherms (full circles) of Fig. 2c. Vapor sorption data for high activities and temperatures in the first sorption run have not been reported since they were not described by ordinary Fick's laws. An explanation of such anomalous behaviour will be given further on using the arguments discussed in the section on sorption model.

Moisture sorption and desorption kinetics for two different values of activity in "as cast" epoxy resin (first sorption - desorption cycles) are reported in Figure 8 for tests made at $T = 75^{\circ}\text{C}$. According to ordinary Fickian diffusion with constant diffusion coefficient (37), both an initial linear part in a weight gain VS \sqrt{t} plot and sorption and desorption data lying on the same curve are

expected. However, while this is verified at low activities ($a = 0.60$ in Fig. 8), at high activities ($a = 0.80$) anomalous behaviour has been found. As previously discussed, the effect of damaging process on the effective diffusion coefficient may be attributed to morphological changes in form of microcavities. The anomalous behaviour shown at high humidity environments could, in principle, be also explained by an actual concentration dependency of diffusion coefficients.

Sorption and desorption tests performed at the same high activity ($a = 0.80$) and temperature on a sample previously equilibrated at $a = 0.99$ (second cycle runs), are shown in Fig. 9. A good superposition of the sorption and desorption data may be observed as predicted by the proposed model, since no additional microvoid formation is expected once the material has already been exposed to more severe conditions. In addition, this result indicates that the use of a real concentration dependent diffusion coefficient would not be satisfactory to explain the anomalies found in Figure 8. Moreover, the environmental conditions of $a = 0.60$ and $T = 75^{\circ} \text{C}$ are not able to induce significant micro -

voiding in the resin since evident anomalies have not been found in the sorption curves.

Sorption curves obtained at the same activity, $a = 0.60$ and $T = 75^{\circ}\text{C}$, for an undamaged sample (A) and for a sample previously equilibrated at $a = 0.99$ at the same temperature (B) are shown in Figure 10. It can be observed, as according to equation 8, that the diffusion coefficient of the damaged sample is lower than that of the undamaged specimens ($b > a$). The morphological modification which increases the solubility of the crazed resin, at fixed environmental conditions, lowers the effective diffusion coefficient.

In Figure 11 the ratios between diffusion coefficients obtained in the same experimental conditions, on samples equilibrated in different environmental conditions, are reported as a function of the ratios between the measured solubilities and are compared with equation 8 (full line). The accordance between the experimental data and the theory is fairly good.

As previously reported, the damaging process is not evident at low external humidity levels for all the temperature investigated, and at low temperatures for all relative humidities analyzed. As a consequence, effective diffusion coefficients for the undamaged polymer can be calculated at high temperatures in low humidity environments.

and at low temperatures in all humidity conditions (also liquid water).

Diffusion coefficients for damaged ($T = 60^{\circ}\text{C}$, $a = 0.99$) and undamaged resin have been crossplotted with solubility data, as a function of the reciprocal of the temperature, taken from the data presented in the previous paragraph. As for the solubility data

open triangles in Fig.12, the diffusion coefficients calculated from tests performed both at low temperatures (2° and 20°C) in liquid water and at high temperatures and low activities (referred as undamaged), are also well correlated by a straight line in the Arrhenius plot (open circles in Figure 12). For damaged samples lower diffusion coefficients (full circles) and higher solubilities (full triangles) have been found in the range of the temperatures studied. Activation energy for the diffusion process of about 13.5 Kcal/mole has been calculated both for damaged and undamaged samples. The corresponding enthalpy of mixing for both materials has been found to be of -11.9 Kcal/mole.

In conclusion, it has been shown that the effect of temperature and humidity on the epoxy microstructure may be noted both from kinetics and equilibrium data. The nature of the hypothesized damaging process (microcavities formation) is in agreement with the diffusion coefficient depression experimentally found and theoretically predicted by an analysis based on Dual Mode Sorption transport model with completely immobilized trapped species.

Applied stress and damaging process in presence of sorbed moisture.

Crazing has been described as a form of yielding in glassy polymers involving significant cavitation and localized fibrillation and orientation of the material surrounding the cavities (38) which develops a thermodynamic restoring force due to conformational entropy changes of the oriented macromolecules. However, in ordinary conditions crazing is considered irreversible since the weakness of the restoring force as related to the forces required to initiate the cavitation, results in a recovery time scale that is decades longer than the typical initiation time scale. In addition, while cavitation is isotropic in character, the fibrillation and orientation of craze surrounding the cavities is not, and, in fact, its directionality has been described (39) in terms of major principal stress always perpendicular to the craze tip, hence the name normal stress yielding (40).

For these reasons a criterion for crazing based entirely on the first invariant is not adequate, implying that craze formation should be a completely isotropic yielding process. The dependence of craze initiation has

been successfully described in terms of deviatoric stress bias (σ_b) versus the reciprocal of the first-stress invariant (I_1) (40). The stress bias, (i.e. stress vector with magnitude equal to the major shear stress but with direction of the major principal stress), may be viewed as the driving force, and as direction determining component of the stress state, for the fibrillation and orientation step, whereas the first-stress invariant is the cavitation driving force.

In equation form it may be expressed as:

$$\sigma_b \geq A + \frac{B}{I_1}$$

where A and B are temperature-dependent material constants and I_1 is the first-stress invariant which must be positive (dilatational) for cavitation. This suggests that as the stress field becomes non dilatational the cavitation process is the limiting factor, craze becomes increasingly difficult to initiate and shear yielding may be observed as yielding mode (40).

The above criteria may be qualitatively used to investigate the nature of the damaging process associated with

moisture sorption. In fact, if craze formation is invoked to explain apparent solubility changes of samples subjected to different hygrothermal histories, the effects of an externally applied stress field on solubilities may be predicted, considering its influence on the driving force for cavitation, I_1 . Sorbed solvent induced osmotic stresses (41) or differential swelling strains of regions with different crosslinking densities (4,23) produce the "internal" stress field distribution responsible for craze formation. The superposition of an external stress field will favor or decrease the tendency of the material to craze, depending on the variations of the resulting first-stress variant. For example, the application of a tensile stress will increase I_1 and a more crazed (damaged) material should be obtained, while, conversely, the application of a hydrostatic pressure will decrease I_1 and a less crazed material should result. Such an expectation has been experimentally tested by performing sorption experiments on samples subjected to different "stress histories" when exposed to the same environmental conditions. Liquid water sorptions have been previously carried out at $T = 40^\circ \text{C}$ on an uniaxially loaded dumbbell sample and on an unloaded reference sample. After a period

three times longer than usually needed to equilibrate unloaded samples at the same temperature, the dumbbell specimens were cut into rectangular shapes and weighed in the wet state. The dry weight was subsequently obtained after a drying procedure under vacuum at $T = 40^{\circ} \text{C}$ until no weight changes were further observed. Weight gains subsequent to resorption from liquid water at $T = 40^{\circ} \text{C}$ were then followed for the two samples with different stress histories, and are reported in Fig. 14. The previously loaded and water penetrated sample clearly shows a higher solubility than the unloaded sample. In Table 1 the applied stress, equilibrium moisture uptakes and percent solubilities increases are reported for the loaded and unloaded samples. An increase of about 16 percent of the apparent solubilities has been found after applying a stress that is only 7 percent of the yielding stress for a saturated sample (42) or 5 percent of the σ break for a dry sample (42). Local yielding in form of crazes may be possible since, for the applied stress used, we are well inside the linear elastic region of the stress-strain curve (42).

The increase in "crazability" expected as a consequence of the increase of the driving force for cavitation, I_1 , is experi-

mentally evident in an apparently higher solubility of the loaded sample.

Concluding, more information on the nature of the damaging process of epoxy resins exposed to humid environments can be obtained performing sorption tests on differently loaded samples at different temperatures. Sorption experiments carried out on samples subjected to hydrostatic compressive stress field are presently in progress. The results will be compared with the previous information on the system as described in this report. The effects of environment on the microstructure will be further developed including "stress histories" in different conditions of temperature and humidity, following the arguments introduced here on the crazing process as a form of local yielding.

REFERENCES

- 1) E.I. Mc Kague Jr, J.E. Halkias and J.D. Reynolds, J. Composite. Mat., 9, 2 (1975)
- 2) Chi - Hung and G.S. Springer, J. Composite Mat., 10, 2 (1976)
- 3) Y. Weitsman, J. Composite Mat., 10, 193 (1976)
- 4) R.J. Morgan and J. O'Neal, J. Mat. Sci., 12, 1966 (1977)
- 5) O. Ishai and U. Arnon, ASTM STP 658, J.R. Vinson Ed. Am. Soc. for Tests. Mat, 1978, pagg. 267-276
- 6) C.E. Browing, Polymer Eng. Sci. 18, 16 (1978)
- 7) A.C. Loos and G.S. Springer, J. Composite. Mat., 12, 17 (1979)
- 8) J.D. Keenan, J.C. Sefaris and J.F. Quinlivan, J. Appl. Polym Sci., in press.
- 9) O. Ishai and U. Arnon, J. of Testing and Evaluation, 5, N. 4, 320 (1977)

- 10) A. Apicella, L. Nicolais, G. Astarita and E. Drioli, Polymer, 20, 9 (1979)
- 11) A.S. Michaels, M.J. Bixler, H.B. Hopfenberg, J. App. Pol. Sci., 12, 991 (1968)
- 12) G.A. Pogany, Polymer, 17, 690 (1976)
- 13) P.G. Le Grand, R.P. Kambour, W.R. Haaf, J. Pol. Sci. A2, 1565 (1972)
- 14) A.C. News, Polymer, 16, 2 (1975)
- 15) T.K. Kwei, H.M. Zupko, J. Pol. Sci., A2, 7, 876 (1969)
- 16) A.R. Berens, H.B. Hopfenberg, Polymer, 19, 489 (1978)
- 17) H.B. Hopfenberg, R.H. Holley, V.T. Stannett, Pol. Eng. Sci. 9, 242 (1969)
- 18) L. Nicolais, E. Drioli, H.B. Hopfenberg, D. Tidone, Polymer, 18, 1137 (1977)
- 19) N. Thomas, A.H. Windle, Polymer, 19, 255 (1978)
- 20) L. Nicolais, E. Drioli, H.B. Hopfenberg, G. Caricati, J. Memb.

- Sci., 2, 231 (1978)
- 21) L. Nicolais, E. Drioli, H.P. Hofferberg and A. Asteolli,
Polymer, 20, 459 (1979)
- 22) R.R. Rambour, E.E. Ramagosa, G.L. Grumer, Macromolecules, 5,
335 (1972)
- 23) U.T. Kreibich, R. Schmid, J.Pol. Sci. Symposium 53, 177 (1975)
- 24) A.S. Kenyon, L.F. Nielsen, J. Macromol. Sci. Chem. A 3 (2),
275 (1969)
- 25) G.A. Gordon, Polymer, 18, 958 (1977)
- 26) A.C. Loos, G.S. Springer, J.Comp. Mat., 13, 17 (1979)
- 27) E.I. Mc Kague, Jr. J.E. Reynolds, J.E. Halkias, J. App. Pol.
Sci., 22, 1643 (1978)
- 28) V.T. Stannet, W.S. Koros, D.R. Paul, H.K. Lonsdale and R.W.
Baker, in Advances in Polymer Science, H.J. Cantow, G.
Dall'Asta, K. Dusek, J.D. Ferry, H. Fujita, M. Gordon, W. Kern,
S. Okamura, C.G. Overberger, T. Saegusa, G.V. Schulz, W.P.
Slichter, J.K. Stille (eds); Springer- Verlag Berlin 1979

- 29) W.H. Vieth, J.M. Howell, J.H. Husein, J. Memb. Sci., 1, 177
(1976)
- 30) G.H. Shen and G.S. Springer, J. Composite Mat., 1, 36 (1976)
- 31) E.L. Mc Kague, Jr., J.D. Reynolds and J.E. Halkias, J. Eng.
Mat. Techn., 48, H, 92 (1976)
- 32) W.R. Vieth, K.J. Sladek, J. Coll. Sci, 20, 1014 (1965)
- 33) D.R. Paul, W.J. Koros, J. Poly. Sci. Phys. Ed., 14, 675 (1976)
- 34) J.H. Petropoulos, J. Poly. Sci., A2 (8), 1797(1970)
- 35) A.S. Michaels, W.R. Vieth, J.A. Barrie, J. Appl. Phys., 24, 13
(1963)
- 36) K.J. Illers, Makromol. Chem., 127, 1 (1969)
- 37) J. Crank, The Mathematics of Diffusion, Oxford Univ. press 1975
- 38) R.P. Kanbour, Macromol. Rev. 7, 1 (1973)
- 39) S.S. Sternstein, L. Ongchin, A. Silverman, Appl. Pol. Symp. 7,
175 (1968)

- 40) S.S. Sternstein, L. Ungchinn, Pol. Prep. 10 ,1117 (1969)
- 41) G. C. Sarti, Polymer 20, 827 (1979)
- 42) L. Nicolais, E. Drioli, A. Apicella, O. Albanese, Int.
Scientific Rep. AFORS 77 - 3369 - 01 (1978).

LIST OF FIGURES

Figure 1. - First (a) and second (b) sorption - desorption weight gain experiments as function of time at different activities and at $T = 60^{\circ}\text{C}$. (c) Equilibrium solubility isotherms at $T = 60^{\circ}\text{C}$ from : first (O) ; second (●) and third (▲) sorption - desorption cycle sets .

Figure 2. - First (a) and second (b) sorption - desorption weight gain experiments as function of time at different activities and at $T = 75^{\circ}\text{C}$. (c) Equilibrium solubility isotherms at $T = 75^{\circ}\text{C}$ from: first (O) and second (●) sorption - desorption cycle sets. Dotted line refers to the initial linear isotherm in the undamaged system .

Figure 3. - First (a) and second (b) sorption - desorption weight gain experiments as function of time at different activities and at $T = 45^{\circ}\text{C}$. (c) Equilibrium solubility isotherms at $T = 45^{\circ}\text{C}$ from : first (O) and second (●) sorption - desorption cycle sets.

Figure 4. - First (a) and second (b) sorption - desorption weight gain experiments as function of time at different activities and at $T = 30^{\circ}\text{C}$. (c) Equilibrium solubility isotherms at $T = 30^{\circ}\text{C}$ from : first (O) and second (●) sorption - desorption cycle sets.

Figure 5. - Weight gains as function of time for water sorption from liquid phase at $T = 20^{\circ}\text{C}$ and $T = 2^{\circ}\text{C}$.

Figure 6. - Equilibrium solubility isotherms as function of the actual moisture pressure.

Figure 7. - Apparent Henry's constants as a function of $1/T$ obtained. From: linear isotherms of second sorption experiments (damaged material) (●); initial linear isotherms of specimens previously equilibrated at $T = 60^{\circ}\text{C}$ and $a = 0.99$, (▲).

Figure 8. - Sorption Kinetics at different humidity levels at $T = 30^{\circ}\text{C}$ (a) and $T = 45^{\circ}\text{C}$ (b) of specimens previously equilibrated at $T = 60^{\circ}\text{C}$ and $a = 0.99$. (c) Comparison between linear isotherms at $T = 45^{\circ}\text{C}$ and $T = 30^{\circ}\text{C}$ for samples equilibrated at the test temperature (●), and previously equilibrated at $T = 60^{\circ}\text{C}$ and $a = 0.99$ (O).

Figure 9. - Moisture sorption (O) and desorption (●) curves for "as cast" resin at two different external activities. $T = 75^{\circ}\text{C}$.

Figure 10. - Moisture sorption (O) and desorption (●) curves for a previously equilibrated resin at $T = 75^{\circ}\text{C}$ and $a = 0.99$. External activity $a = 0.80$.

Figure 11. - Comparison between moisture sorption in the same external conditions for resin with different previous histories.

Figure 12. - Diffusion coefficient reductions D'/D'' for solubility increases (K_H / K_H'): (O) experimental, (—) equation 8.

Figure 13. - Crossplot of diffusion coefficients and solubilities as function of $1/T$ for undamaged (O, Δ) and damaged at $T = 60^{\circ}\text{C}$ and $a = 0.99$ (●, \blacktriangle) epoxy resins.

Figure 14. - Liquid water uptake in resorption tests performed on previously saturated in liquid water and subsequently dried samples ($T = 40^{\circ}\text{C}$). (O) Previously loaded ($= 0.30 \text{ kg/mm}^2$) and (●) unloaded samples.

TABLE 1

$\sigma, \text{kg/mm}^2$	$C, \text{g solv/100g dry pol.}$	$\Delta C, \%$
0	3.89	0
0.20	4.54	16.3

Table 1: apparent solubility differences between loaded and unloaded samples exposed to liquid water at $T = 40^\circ\text{C}$.

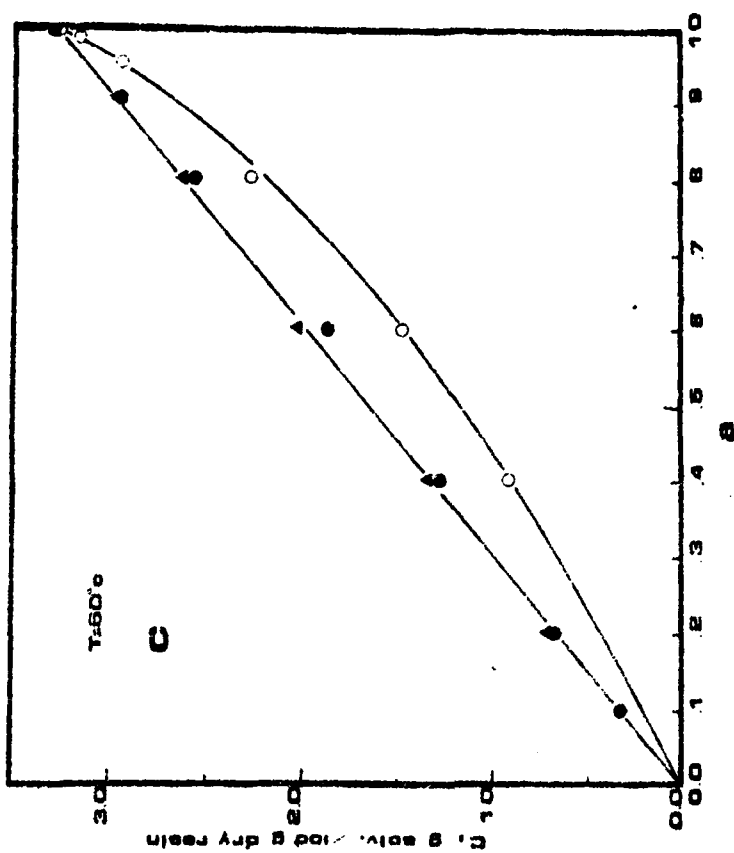
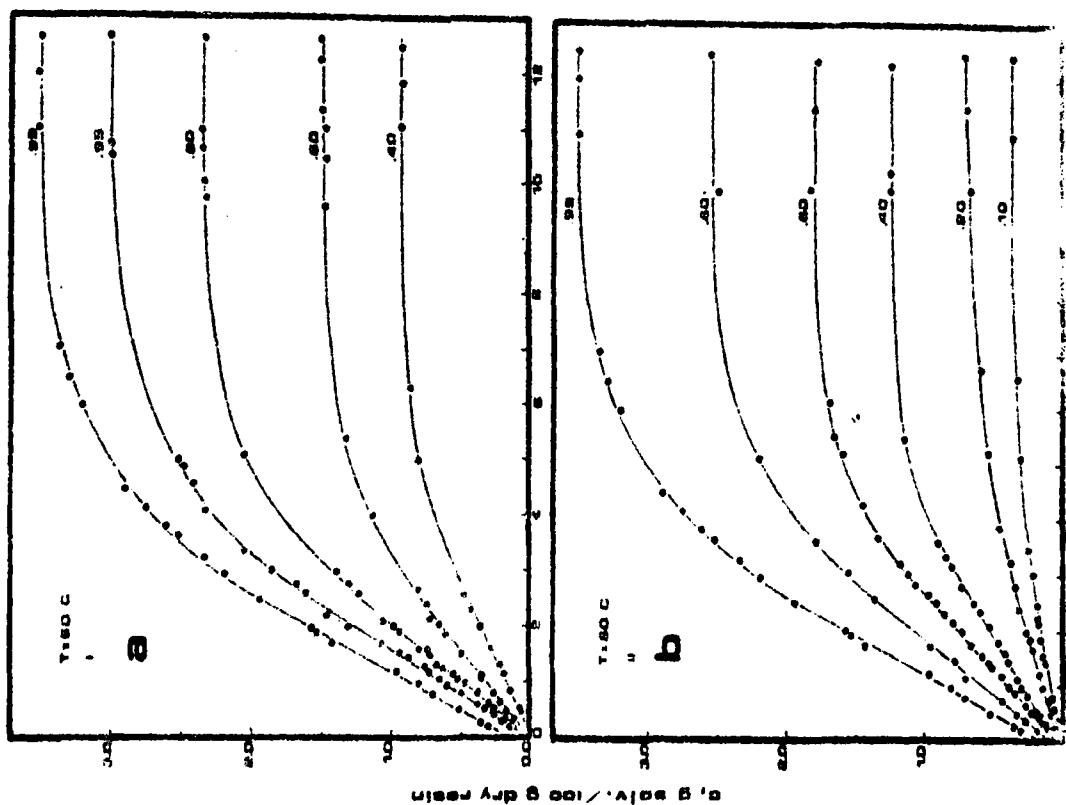


Figure 1. - First (a) and second (b) sorption - desorption weight gain experiments as function of time at different activities and at $T = 60^{\circ}\text{C}$. (c) Equilibrium solubility isotherms at $T = 60^{\circ}\text{C}$ from : first (O) ; second (●) and third (▲) sorption - desorption cycle sets .



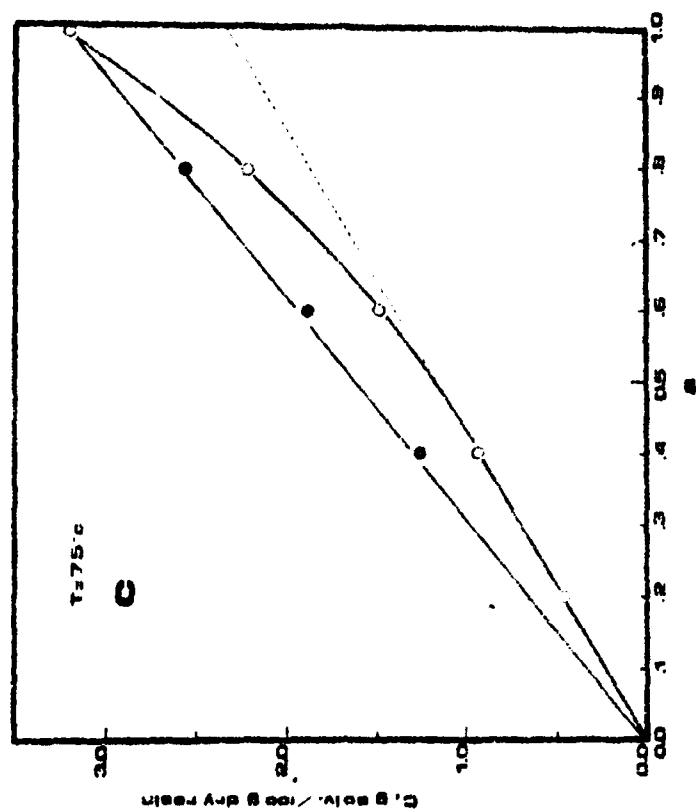
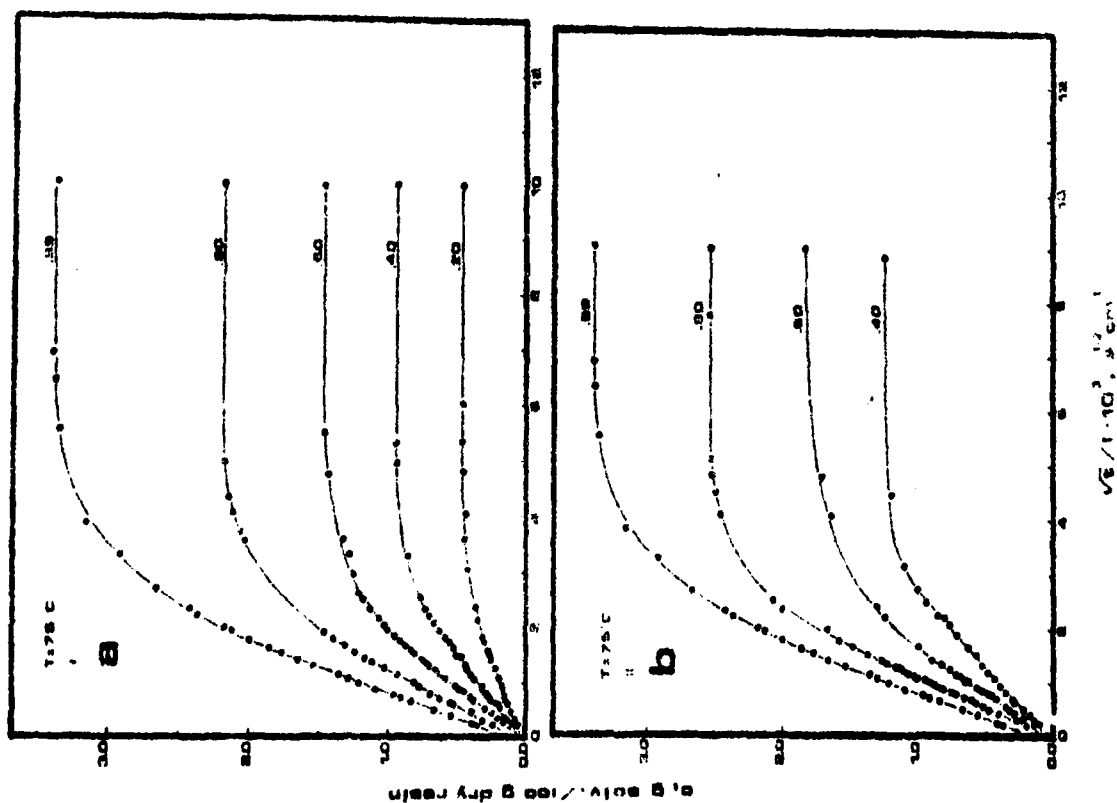


Figure 2. - First (a) and second (b) sorption - desorption weight gain experiments as function of time at different activities and at $T = 75^\circ\text{C}$. (c) Equilibrium solubility isotherms at $T = 75^\circ\text{C}$ from: first (O) and second (●) sorption - desorption cycle sets. Dotted line refers to the initial linear isotherm in the undamaged system.

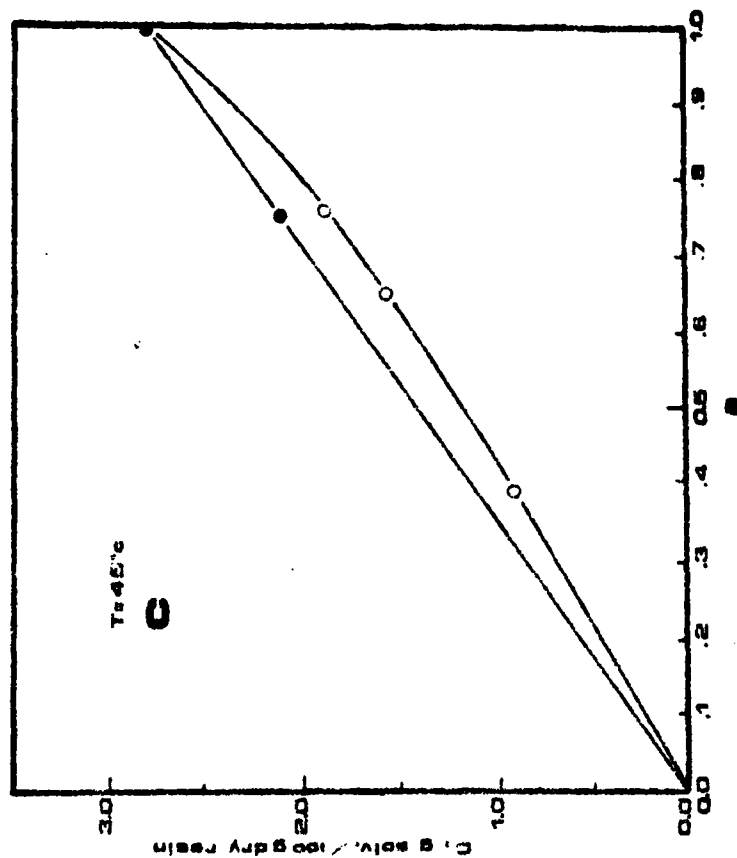
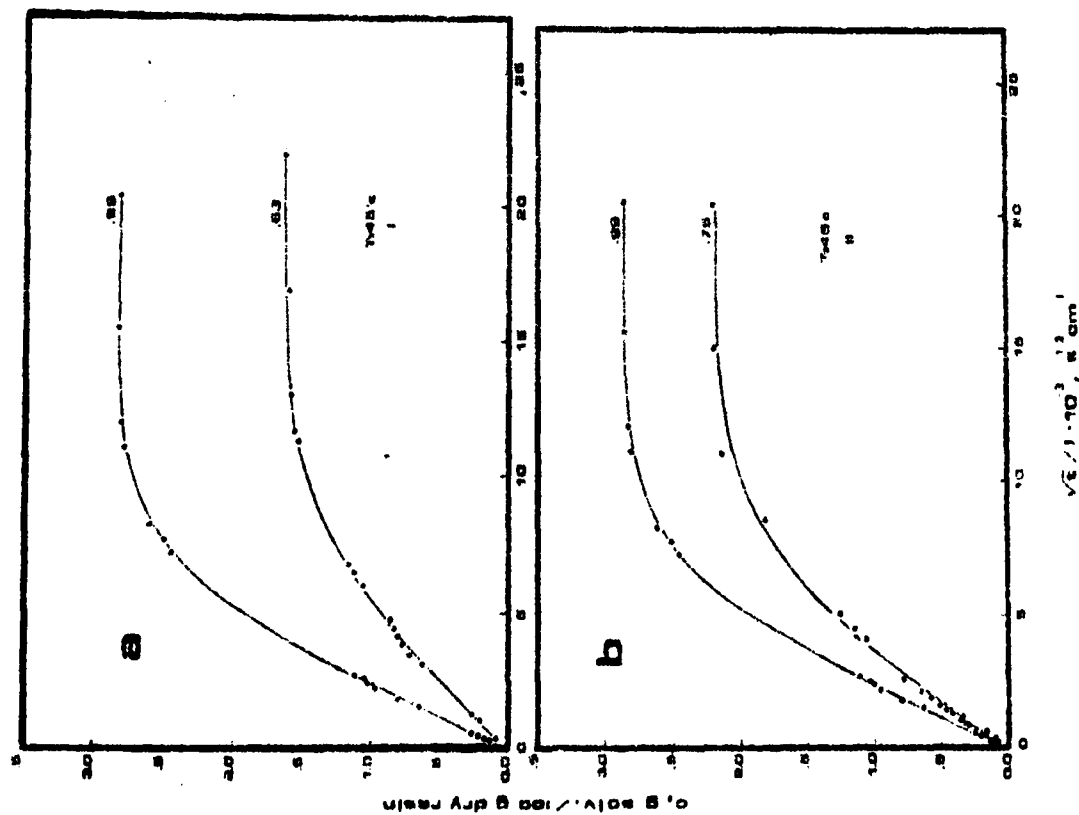


Figure 3. - First (a) and second (b) sorption - desorption weight gain experiments as function of time at different activities and at $T = 45^\circ\text{C}$. (c) Equilibrium sorclivity isotherms at $T = 45^\circ\text{C}$ from : first (O) and second (●) sorption - desorption cycle sets.

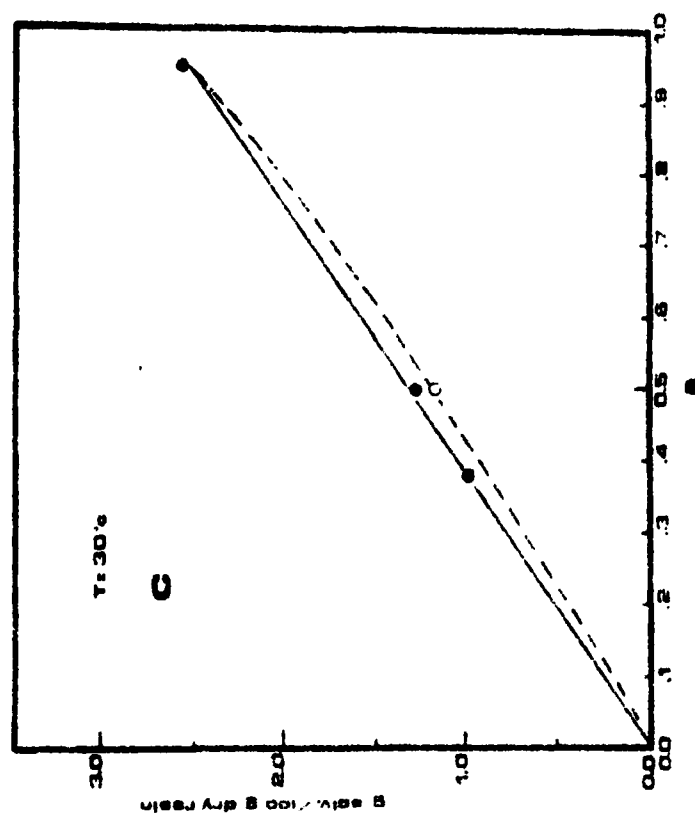
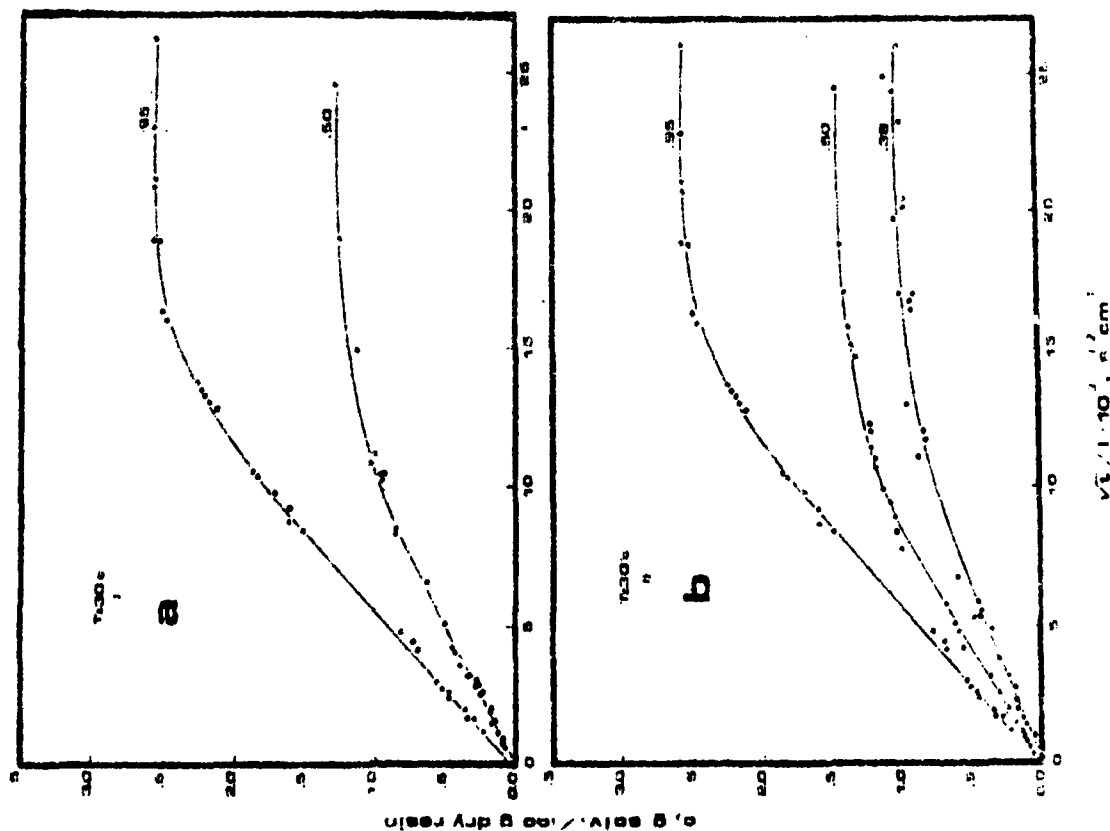


Figure 4. - First (a) and second (b) sorption - desorption weight gain experiments as function of time at different activities and at $T = 30^\circ\text{C}$. (c) Equilibrium solubility isotherms at $T = 30^\circ\text{C}$ from: first (O) and second (●) sorption - desorption cycle sets.

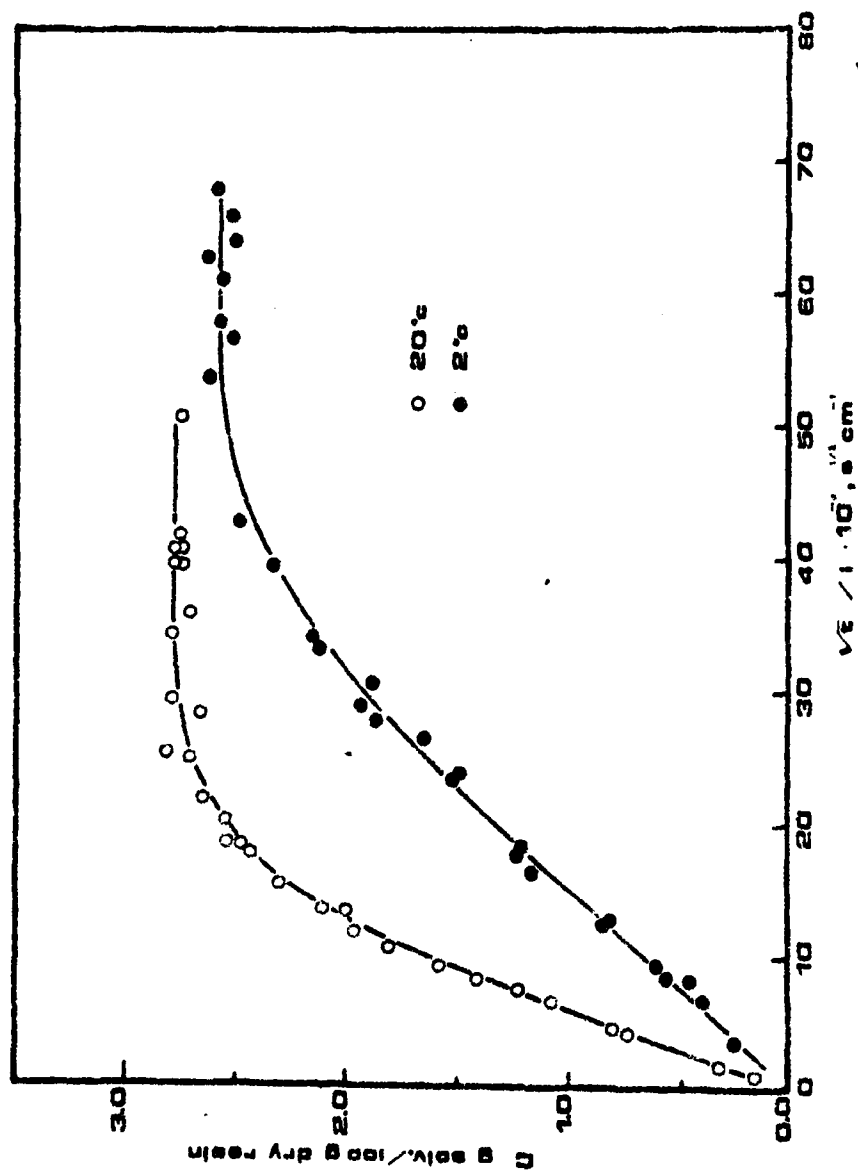


Figure 5. - Weight gain as function of time for water sorption from liquid phase at $T = 20^\circ\text{C}$ and $T = 2^\circ\text{C}$.

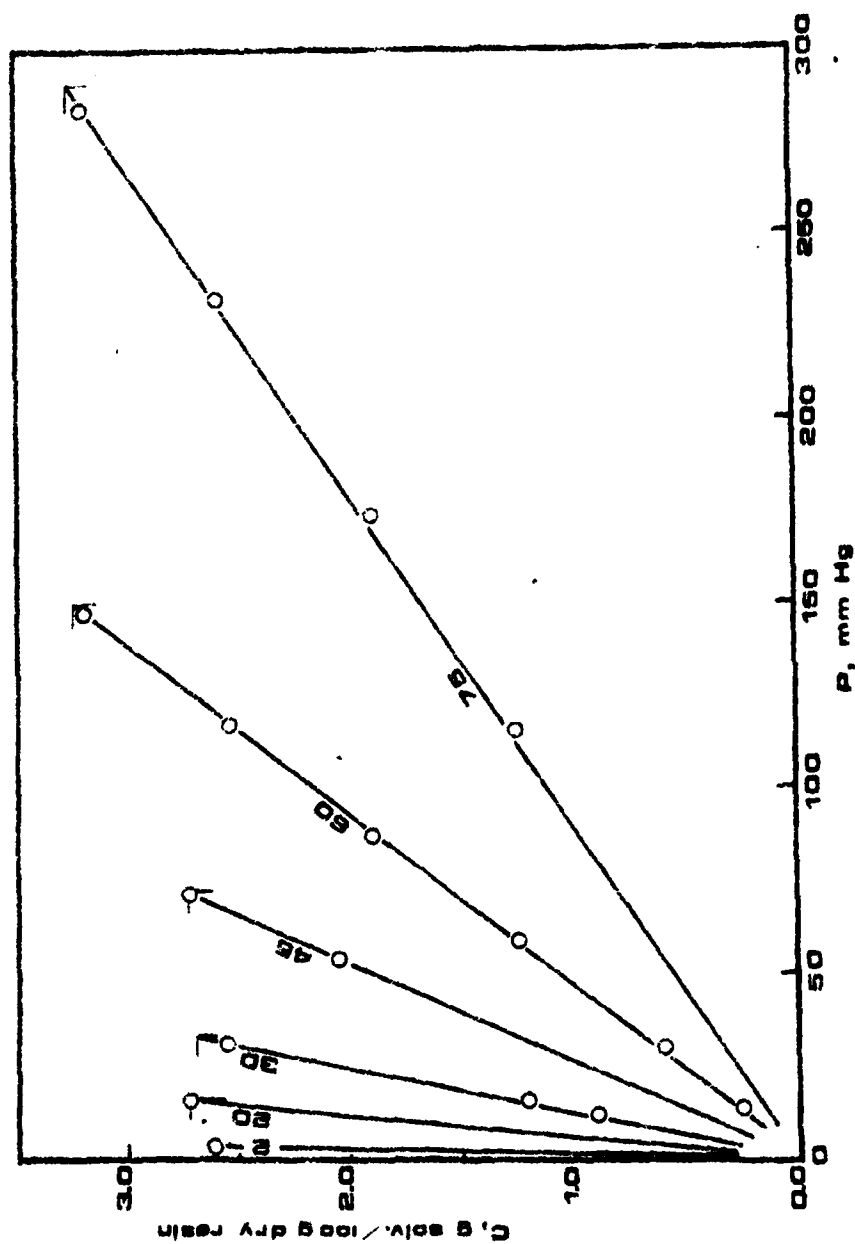


Figure 6. - Equilibrium solubility isotherms as function of the actual moisture pressure.

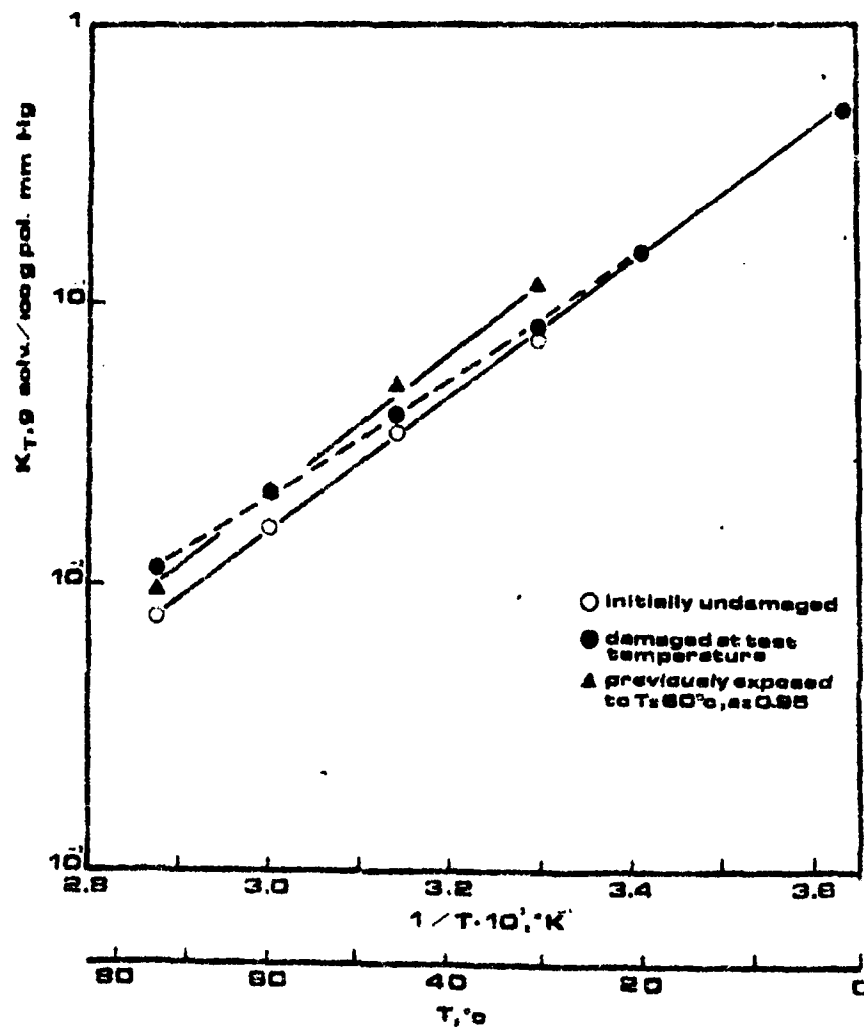


Figure 7. - Apparent Henry's constants as a function of $1/T$ obtained from: linear initial part of upward isotherms (undamaged) (○); linear isotherms (damaged material) (●); linear isotherms of specimens previously exposed at $T = 60^{\circ}\text{C}$ and $a = 0.99$ (▲).

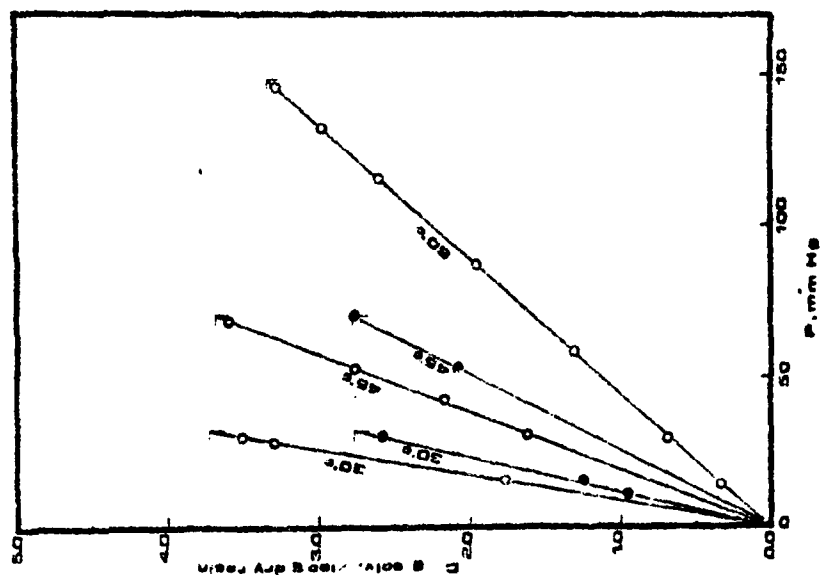
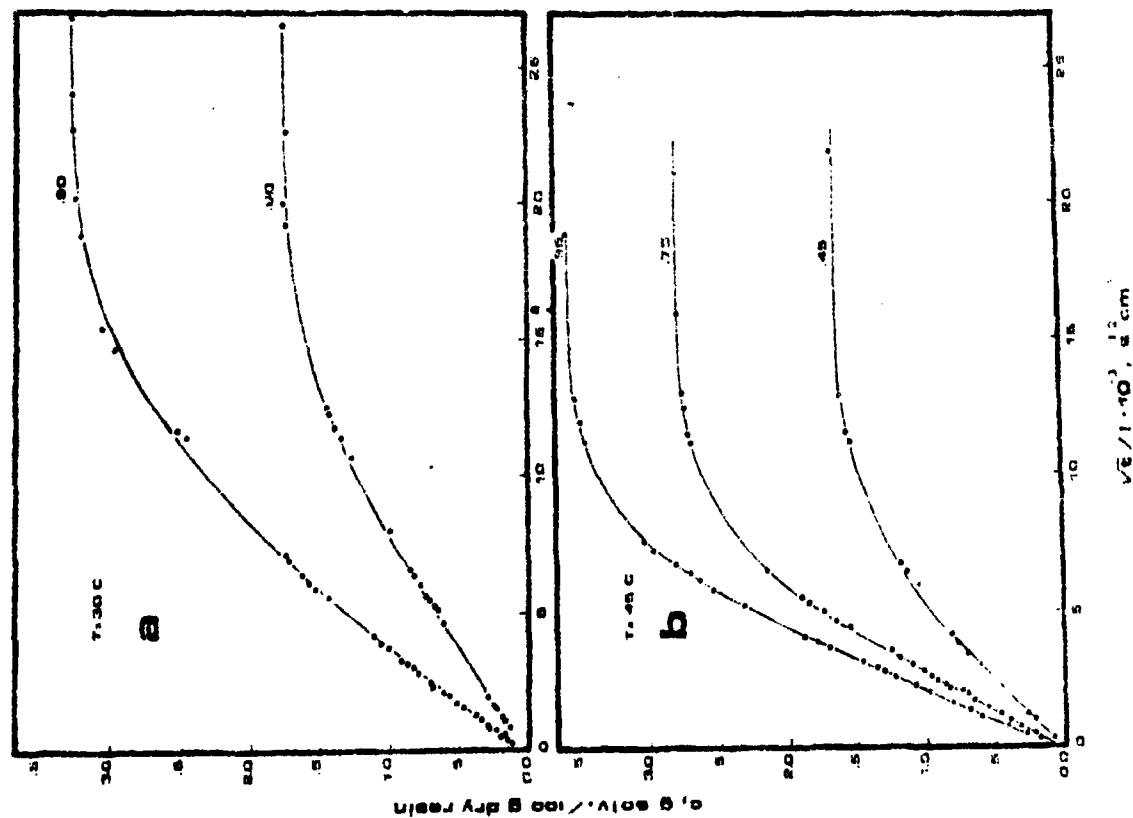


Figure 8. - Sorption Kinetics at different humidity levels at $T = 30^\circ \text{C}$ (a) and $T = 45^\circ \text{C}$ (b) of specimens previously equilibrated at $T = 60^\circ \text{C}$ and $a = 0.99$. (c) Comparison between linear isotherms at $T = 45^\circ \text{C}$ and $T = 30^\circ \text{C}$ for samples equilibrated at the test temperature (●), and previously equilibrated at $T = 60^\circ \text{C}$ and $a = 0.99$ (○).

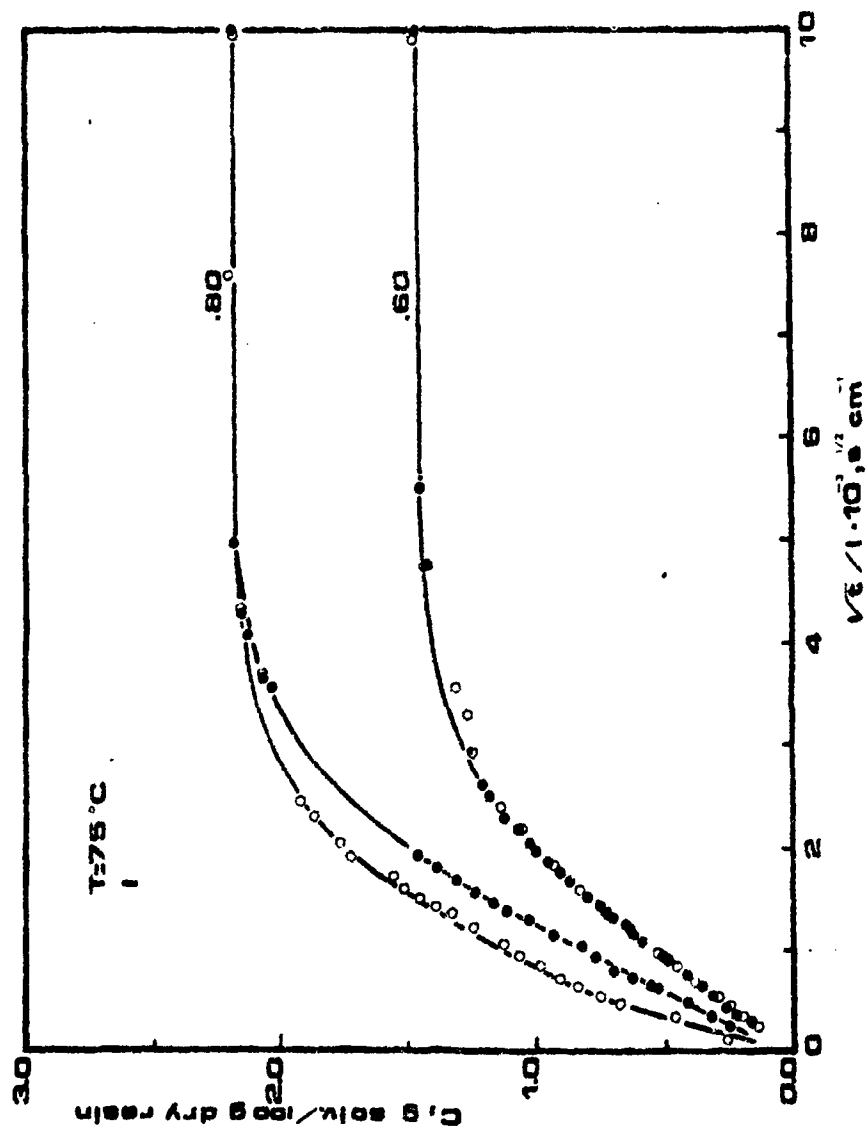


Figure 9. - Moisture sorption (○) and desorption (●) curves for "as cast" resin at two different external activities. $T = 75^{\circ}\text{C}$.

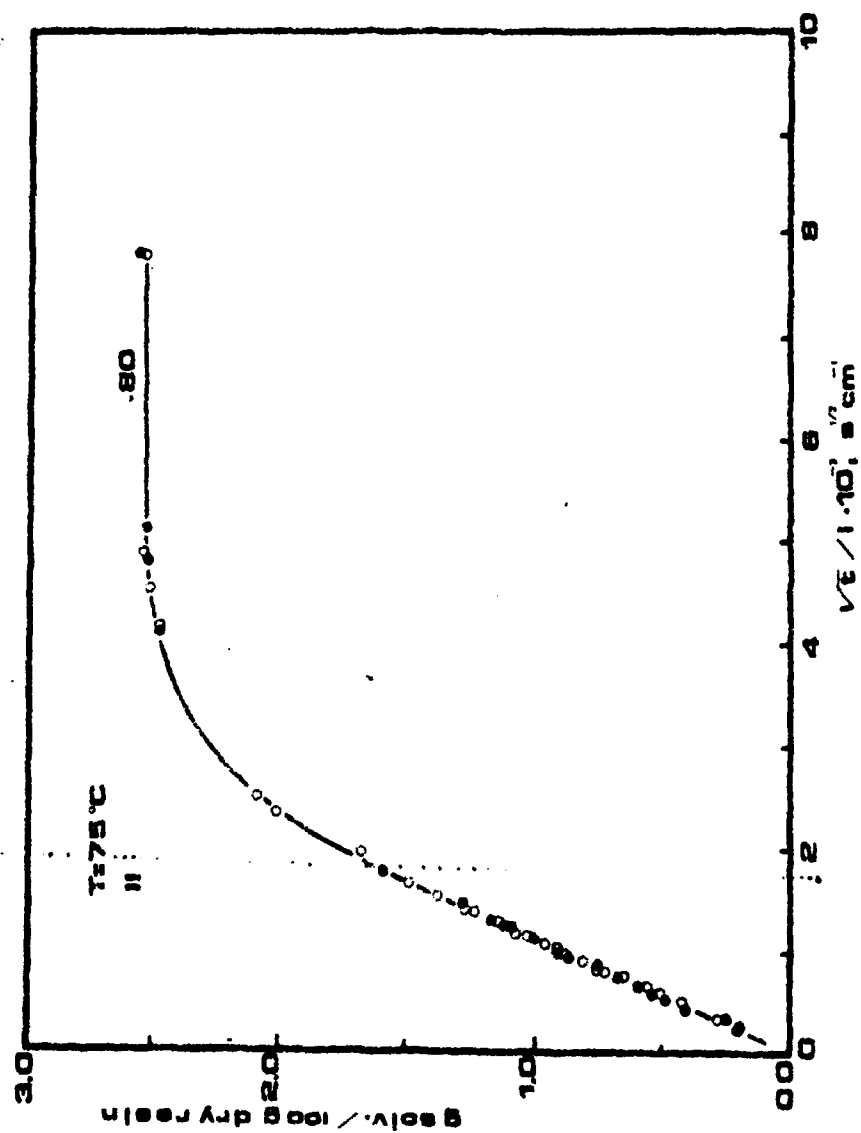


Figure 10. - Moisture sorption (O) and desorption (●) curves for a previously equilibrated resin at $T = 75^\circ\text{C}$ and $a = 0.99$. External activity $a = 0.80$.

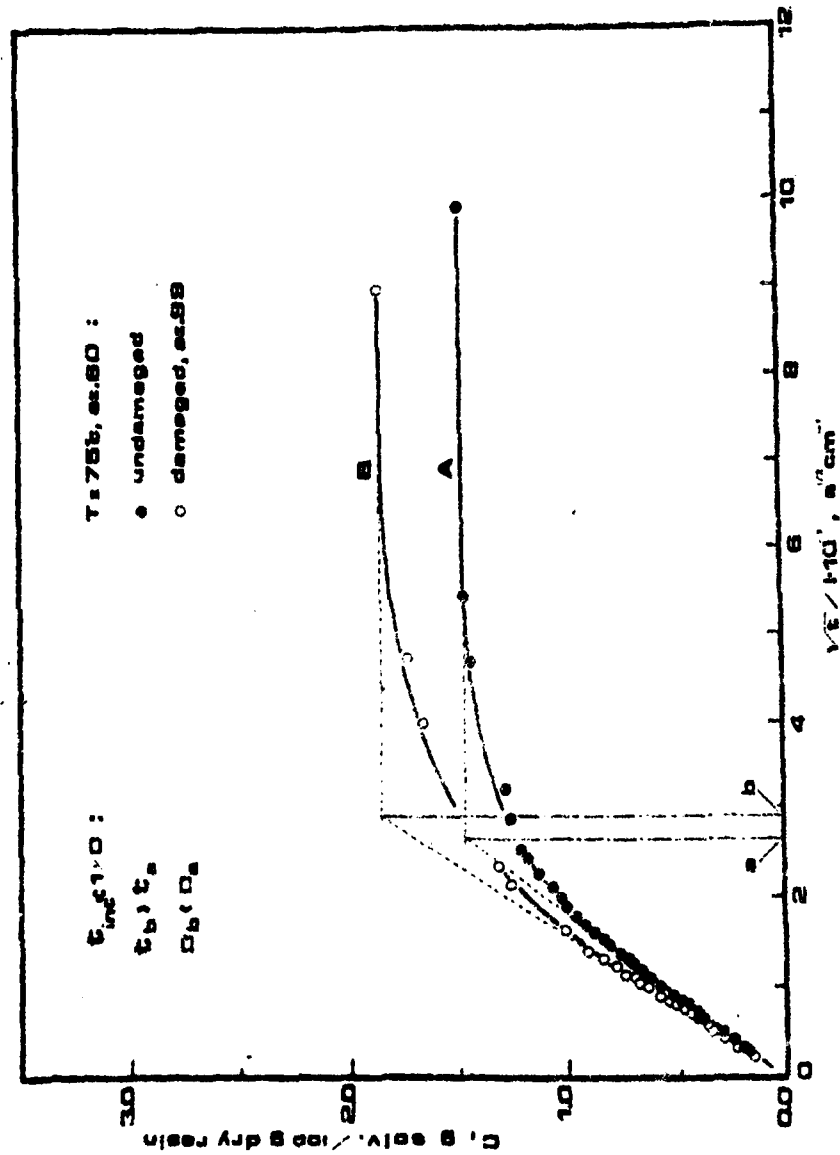


Figure 11. - Comparison between moisture sorption in the same external conditions for resin with different previous histories.

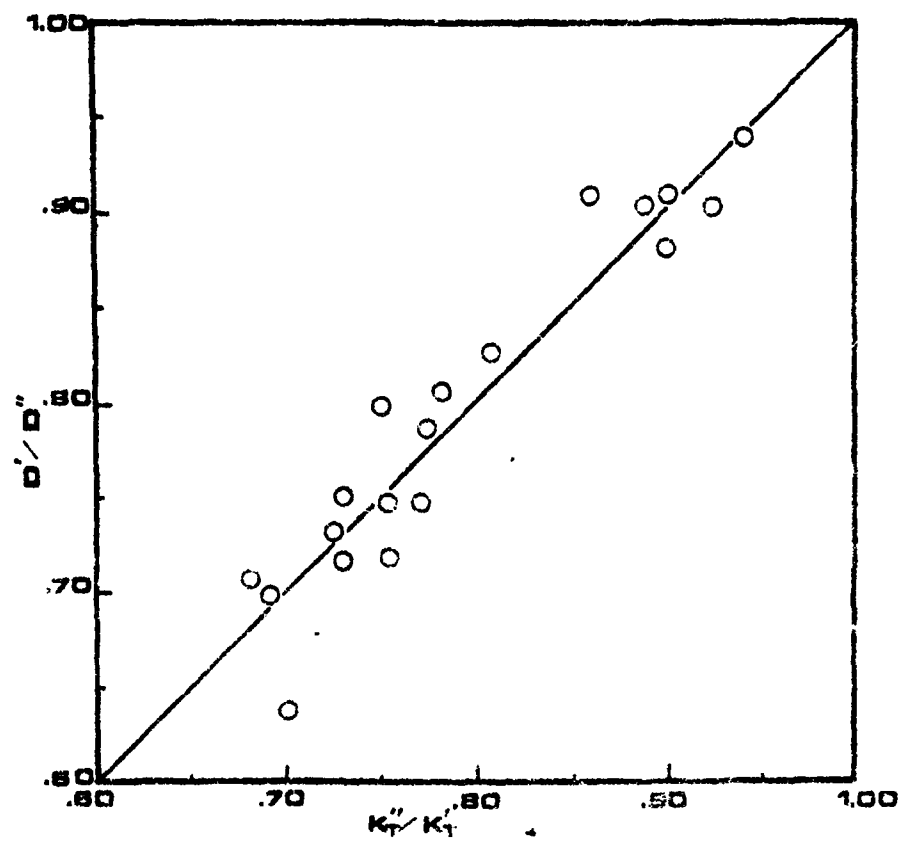


Figure 12. - Diffusion coefficient reductions D'/D'' for solubility increases (K_T''/K_T'): (O) experimental, (—) equation 8.

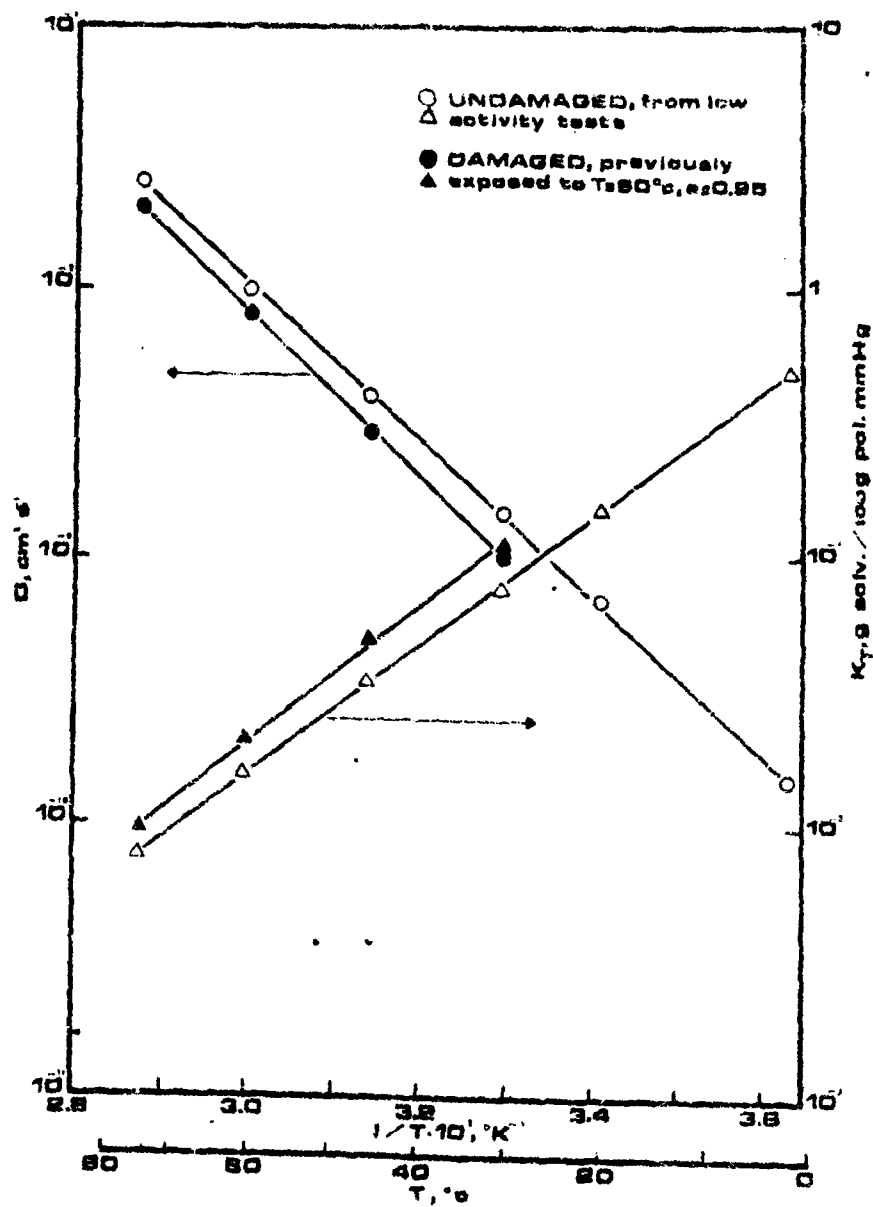


Figure 13. - Crossplot of diffusion coefficients and solubilities as function of $1/T$ for undamaged (○, △) and damaged at $T = 60^{\circ}\text{C}$ and $a = 0.99$ (●, ▲) epoxy resins.

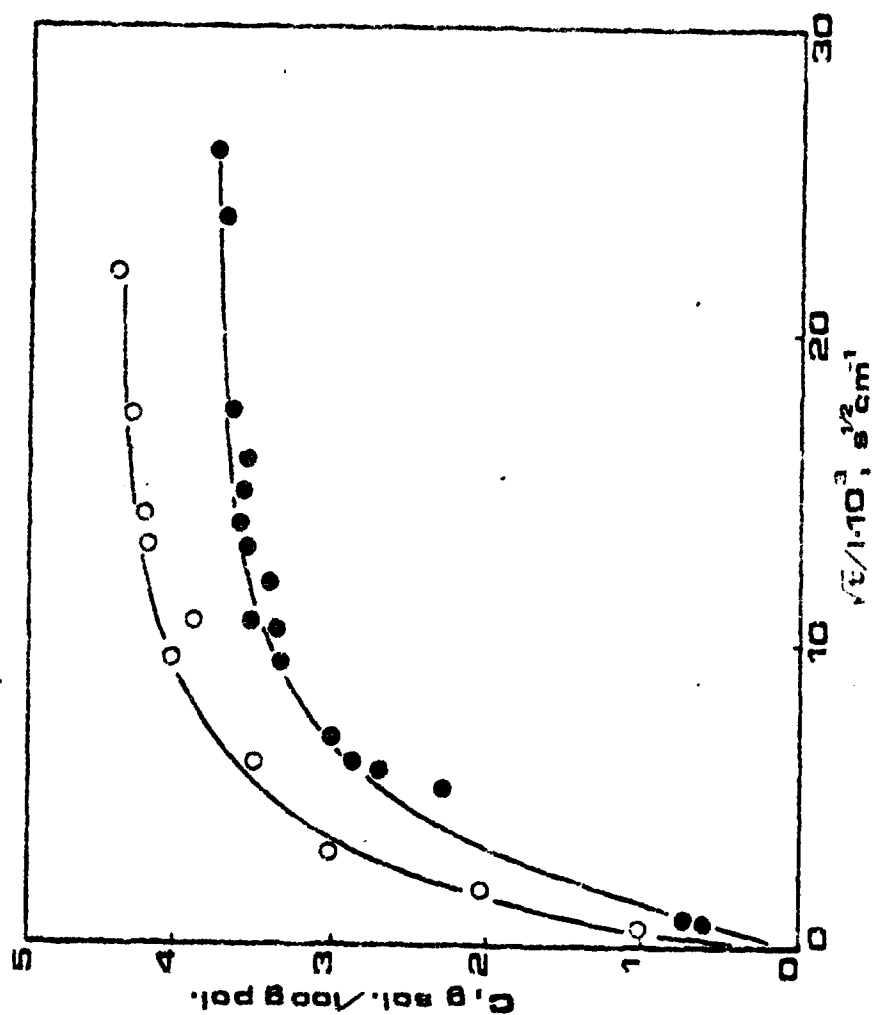


Figure 14. - Liquid water uptake in resorption tests performed on previously saturated in liquid water and subsequently dried samples ($T = 40^\circ\text{C}$). (O) Previously loaded ($= 0.30 \text{ kg/mm}^2$) and (●) unloaded samples.

